

1

Supplementary Information

2 Nitrogen doped carbon fibers coating embedded in the separator 3 for stable zinc batteries

4 Dingzhong Luo,^a Jiae Wu,^a Wentao Deng,^a Guoqiang Zou,^a Hongshuai Hou,^{*a}
5 Xiaobo Ji,^a

6 ^aNational Energy Metal Resources and New Materials Key Laboratory, College of
7 Chemistry and Chemical Engineering, Central South University, Changsha, 410083,
8 China

9 Corresponding Author Email address: hs-hou@csu.edu.cn

10

11 1. Experimental Section

12 1.1. Material Synthesis

13 1.1.1 Synthesis of CDs and Carbon Fibers

14 The synthesis of CDs and carbon fibers was based on our previous reports.¹
15 NaOH (12 g) was gradually added into acetaldehyde solution (40 mL, 40% aqueous
16 solution) under violent stirring, and the resulting mixture was continuously stirred for
17 2 hours. And then, the product was sonicated with diluted hydrochloric acid and water
18 until flocculation occurred. Subsequently, the product underwent washing with
19 deionized water until neutralization was achieved. The resulting CDs were then dried
20 in a drying oven at 70 °C. For the synthesis of carbon fibers, a homogeneous mixture
21 of carbon dots (0.4 g) and zinc chloride (2.4 g) was subjected to heating at 400 °C for
22 4 hours in an argon atmosphere, with a heating rate of 10 °C min⁻¹. The resulting
23 calcined product (CF400) underwent washing with diluted hydrochloric acid and
24 distilled water. The dried CF400 was then mixed with carbamide, followed by heating
25 to 700 °C at a temperature rising rate of 3 °C min⁻¹ under argon, and maintained for 2
26 hours. The washing and drying procedures for nitrogen-doped carbon fibers (NCF700)
27 were identical to those for CF400. The synthesis of pure carbon fibers (CF700)
28 followed the same process as NCF700, except for the absence of carbamide.

29 1.1.2 Preparation of modified separator

30 The coated separator was fabricated by blending carbon fibers (CF700 or
31 NCF700) and carboxymethyl cellulose (CMC) at a mass ratio of 8:2 in an appropriate
32 quantity of deionized (DI) solvent. Following magnetic stirring for 12 hours at room
33 temperature, the resulting homogeneous slurry was applied onto a glass fiber
34 separator using the doctor blading technique. Subsequently, the coated separator was
35 subjected to vacuum drying at 60 °C for 12 hours to eliminate excess water solvent,
36 yielding the products termed CF700@GF or NCF700@GF. After obtaining the dried
37 composite separator, it is cut into circular pieces of uniform diameter. Subsequently,
38 these separator pieces, laden with identical loads of carbon fiber, are assembled
39 together in a coated juxtaposition manner to form the composite separator. This
40 resultant structure is designated as GF@CF700@GF and GF@NCF700@GF. Two
41 pieces of separator with the same size were assembled with their coated sides facing

42 the electrode and designated as GF@GF@NCF700. The blank control group employs
43 two uncoated separator pieces for identical assembly procedures, designated as
44 GF@GF. In all electrochemical tests conducted in this paper, bilayer assembled
45 separators were utilized.

46 1.1.3 Preparation of Mg-Doped $\text{NH}_4\text{V}_4\text{O}_{10}$ (MNVO) cathode materials

47 The MNVO was synthesized using a modified hydrothermal method as described
48 in previous literature.² $\text{NH}_4\text{V}_4\text{O}_{10}$ was synthesized through a single-step hydrothermal
49 method, wherein 0.64 g NH_4VO_3 was dissolved in 80 ml of deionized (DI) water at 60
50 °C with stirring. Subsequently, 1.16 g $\text{H}_2\text{C}_2\text{O}_4 \cdot 2\text{H}_2\text{O}$ was added to the solution until it
51 attained a dark green color. Upon complete dissolution, magnesium oxalate was
52 introduced into the dark green solution at a predetermined ratio (Mg:V = 1:16). The
53 resulting mixture was transferred to a 100 ml Teflon-lined autoclave and maintained
54 at 180 °C for 3 hours. The resulting dark green powder was obtained by successive
55 rinsing with distilled water/alcohol and subsequent vacuum drying at 60 °C for 24
56 hours. The MNVO cathodes were prepared by blending 60 wt% of active materials,
57 20 wt% of polyvinylidene fluoride (PVDF) binder, and 20 wt% of conductive carbon
58 (Super P) in N-methyl pyrrolidinone (NMP). These slurries were then coated onto
59 stainless-steel mesh substrates containing the active materials. Finally, the prepared
60 electrodes were obtained for further use after vacuum drying at 100 °C for 10 hours.

61

62 2. Materials Characterizations

63 X-ray diffraction (XRD) data were acquired using a Rigaku Ultima IV X-ray
64 diffractometer operating at a scan rate of 10°min^{-1} . High-resolution transmission
65 electron microscopy (HRTEM), elemental mapping, and selected-area electron
66 diffraction (SAED) patterns were obtained using a JEOL JEM 2100F transmission
67 electron microscope (TEM). The scanning electron microscope (SEM) images of the
68 separators and carbon fibers were captured using a JEOL JSM-7610F Plus and a
69 TESCAN MIRA4. Optical images of the electrodes were acquired using a Digital
70 Microscope KH-7700. Contact angle measurements between the
71 GF@GF/GF@NCF700@GF and the 2 M ZnSO_4 electrolyte were performed using a
72 Contact Angle Goniometer (SDC-100 China, Dongguan). Electron probe
73 microanalysis (EPMA) was conducted using a JXA152 8530F-PLUS instrument.

74

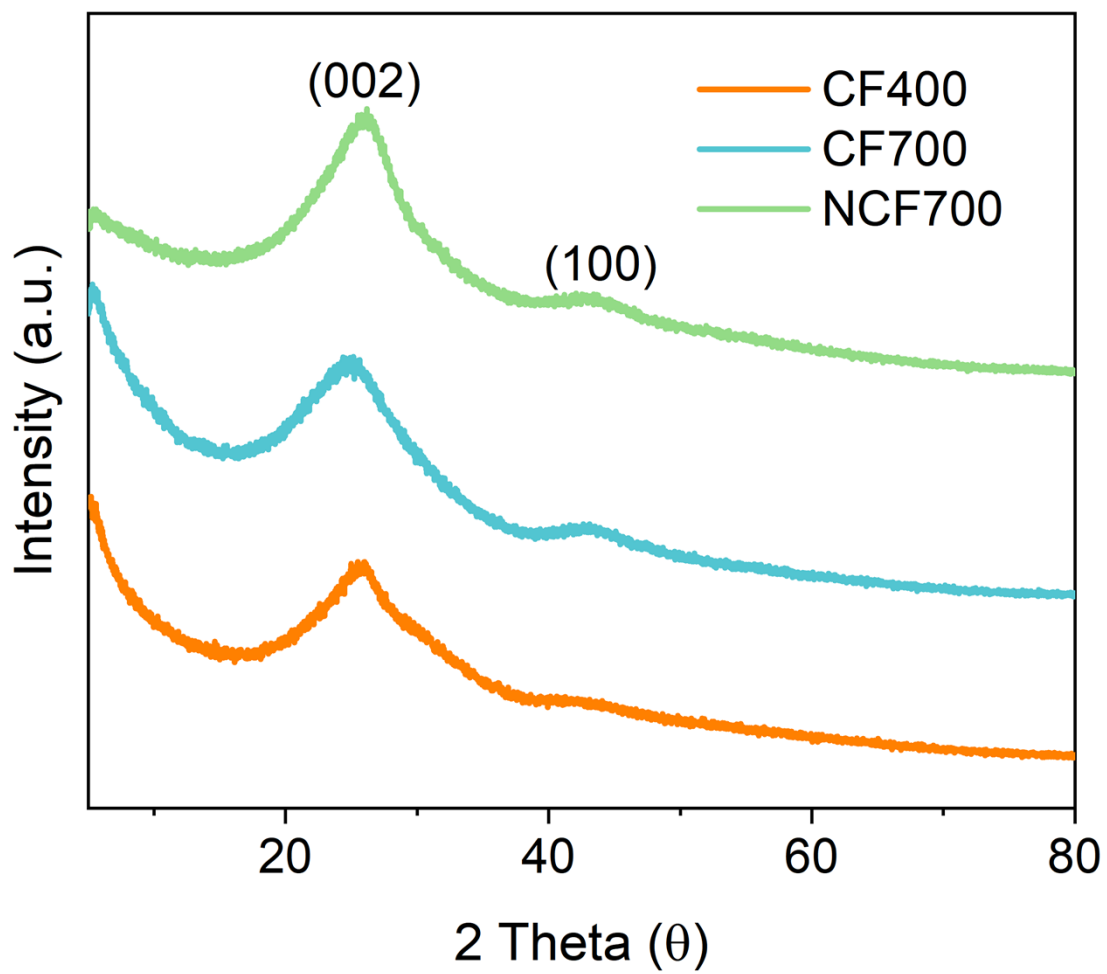
75 3. Electrochemical measurements

76 All experiments were conducted using CR2016 coin cells, employing GF@
77 GF/GF@CF700@GF/GF@NCF700@GF separators and a 2 M ZnSO_4 electrolyte.
78 Electrodes were shaped into circular disks with a diameter of 12 mm. Symmetric cells
79 were constructed using two identical disks, resulting in both the anode and cathode
80 being identical. Half cells were assembled using two different disks, with the anode
81 being a bare Zn anode and the cathode a bare Cu electrode. Assembly of
82 $\text{Zn}||\text{GF@GF/GF@NCF700@GF}||\text{MNVO}$ full cells followed a similar procedure to
83 $\text{Zn}||\text{GF@GF/GF@NCF700@GF}||\text{Zn}$ symmetric cells, except one Zn electrode was
84 replaced with an MNVO cathode.

85 Electrochemical characterization, including electrochemical impedance
86 spectroscopy (EIS), cyclic voltammetry (CV), Tafel curves, and Chronoamperometry
87 (CA), was performed using a CHI660E electrochemical workstation. CV analysis of
88 half cells was conducted at a scan rate of 1 mV s⁻¹, while CV analysis of full cells was
89 conducted at a scan rate of 0.2 mV s⁻¹. Contact angle (CA) measurements were
90 conducted in Zn||GF@GF/GF@NCF700@GF||Zn symmetric cells at an overpotential
91 of -150 mV. The electrochemical performance of Zn||GF@GF||MNVO and
92 Zn||GF@NCF700@GF||MNVO full cells was assessed using a Neware BTS4000 test
93 system within a voltage window of 0.2 to 1.5 V.

94

95

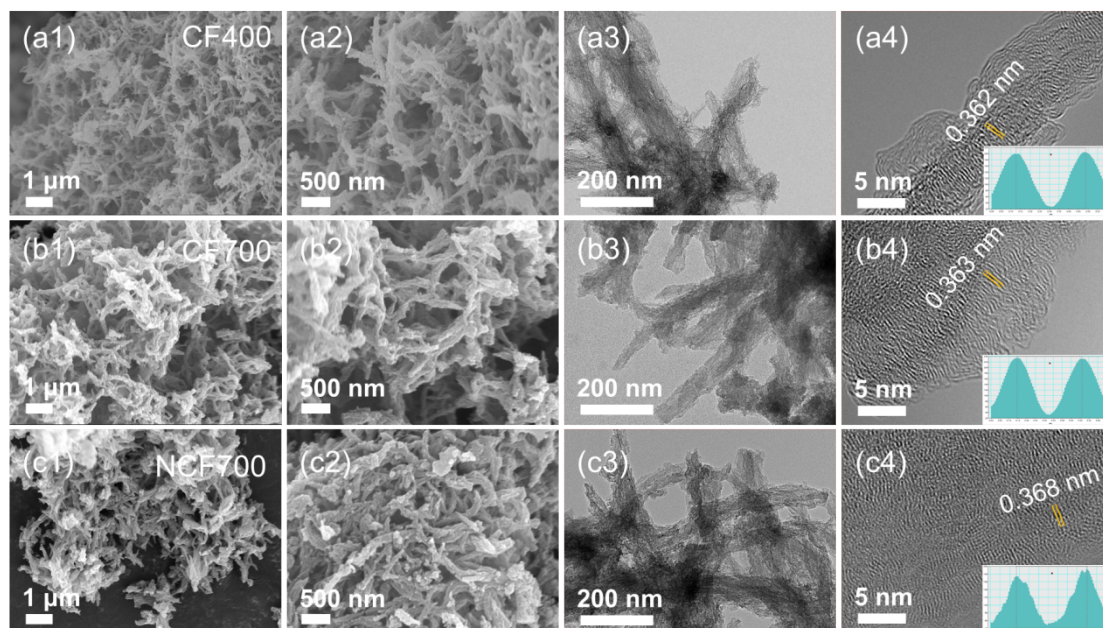


96

97 Fig. S1 XRD patterns of CF400, CF700 and NCF700.

98

99

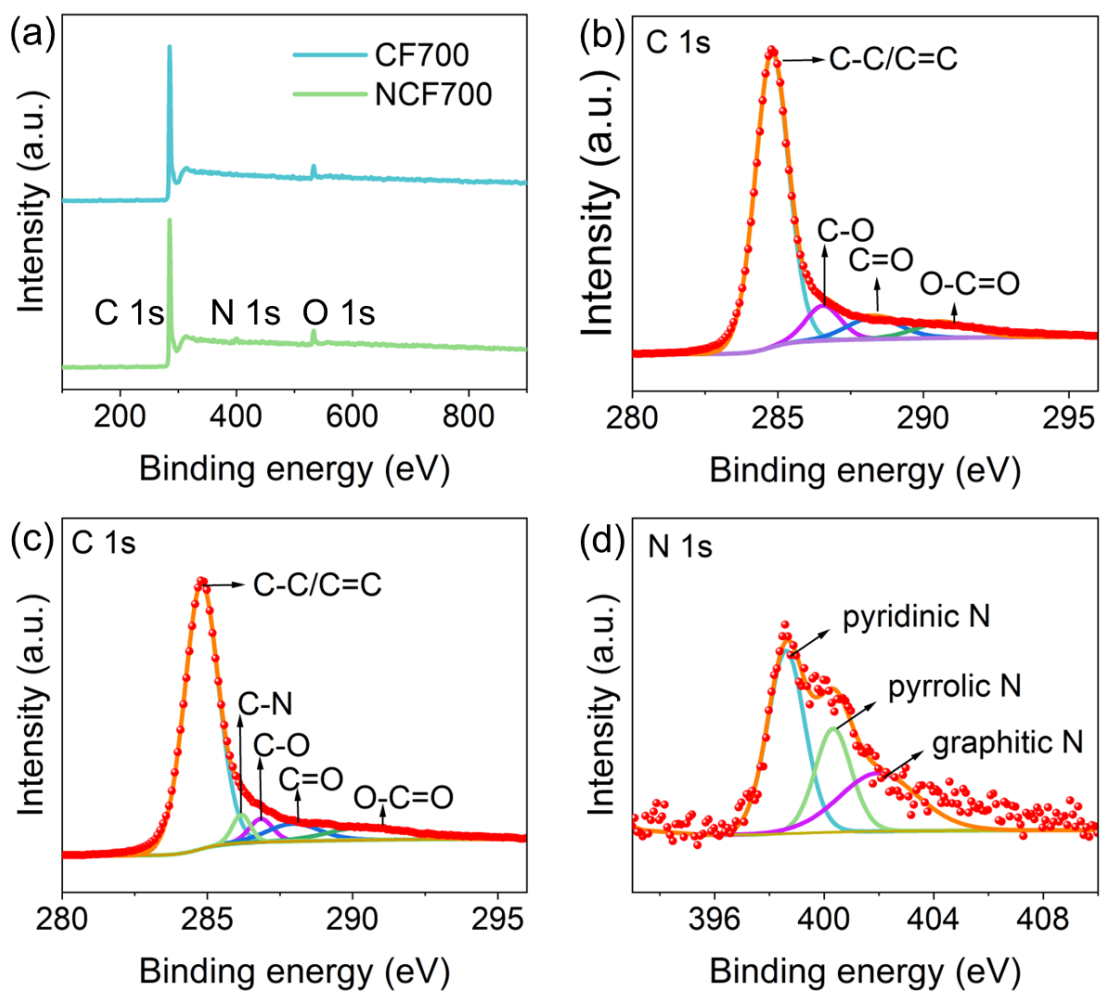


100

101 Fig. S2 SEM, TEM, and HRTEM of (a) CF400, (b) CF700, and (c) NCF700.

102

103

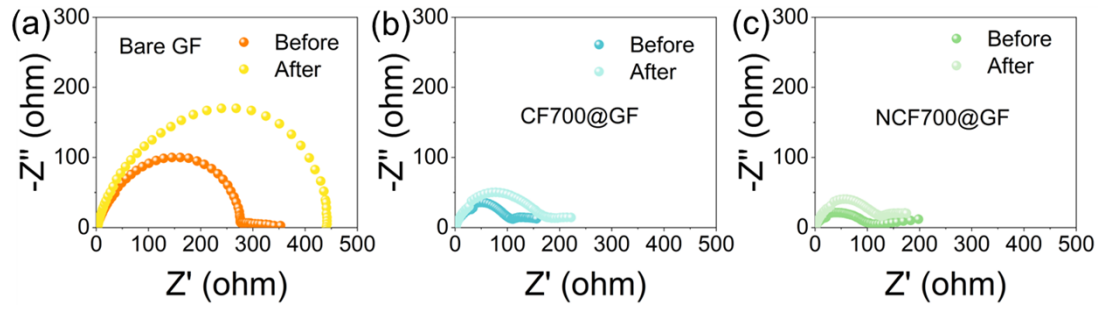


104

105 Fig. S3 (a) XPS survey spectra, The C 1s spectra of (b) CF700 and (c) NCF700, (d)

106 high-resolution N 1s of NCF700.

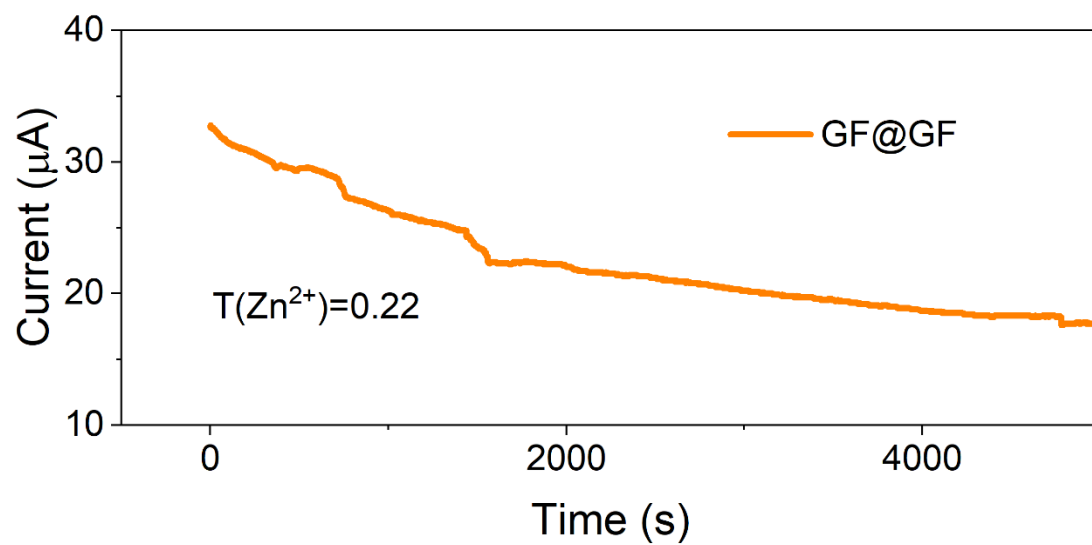
107



108

109 Fig. S4 Nyquist plots of symmetric cells with (a) bare GF, (b) CF700@GF and (c)
 110 NCF700@GF separators before and after CA measurement.

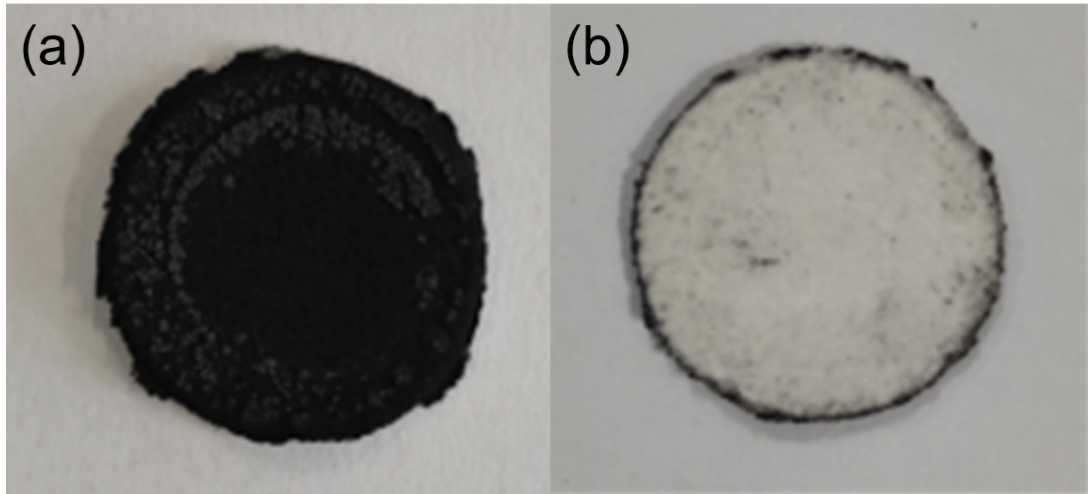
111



112

113 Fig. S5 Chronoamperometric curve of symmetric batteries with GF@GF separator.

114

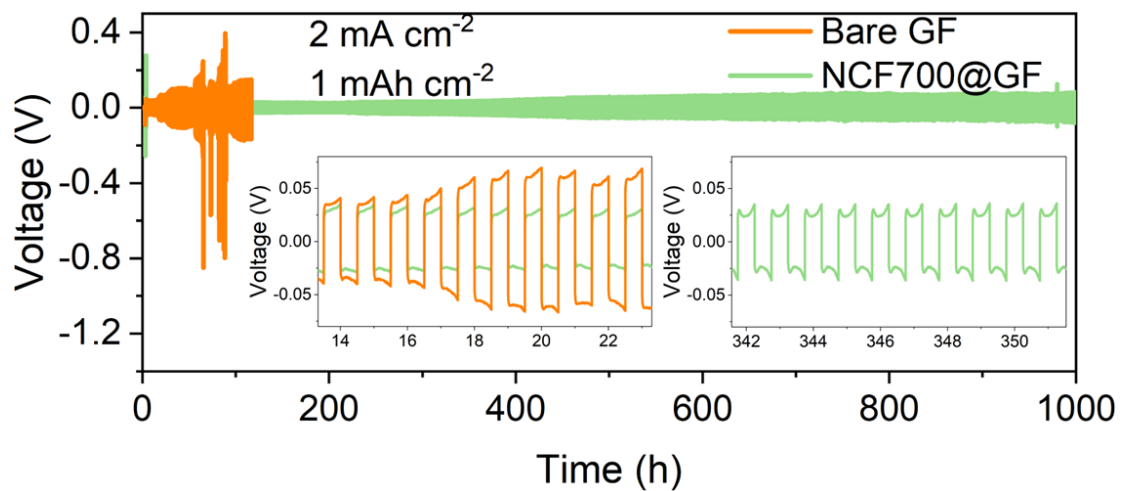


115

116 Fig. S6 digital photos of NCF700@GF FZM (a) and NCF700@GF (b) separator after
117 20 cycles at 4 mA cm^{-2} and 4 mAh cm^{-2} .

118

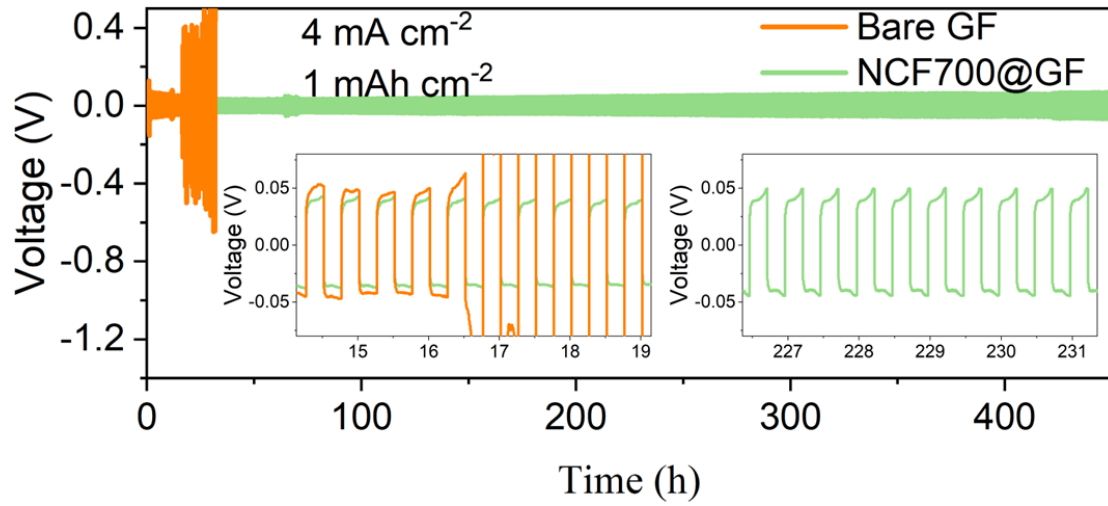
119



120

121 Fig. S7 Cycling performance of symmetric batteries based on bare GF and
122 NCF700@GF at 2 mA cm^{-2} .

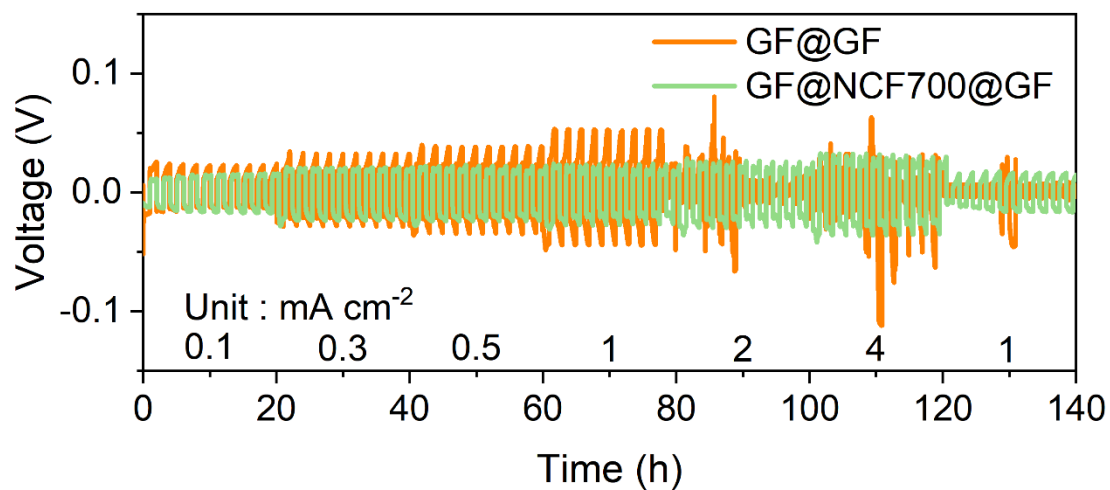
123



124

125 Fig. S8 Cycling performance of symmetric batteries based on bare GF and
126 NCF700@GF at 4 mA cm^{-2} .

127



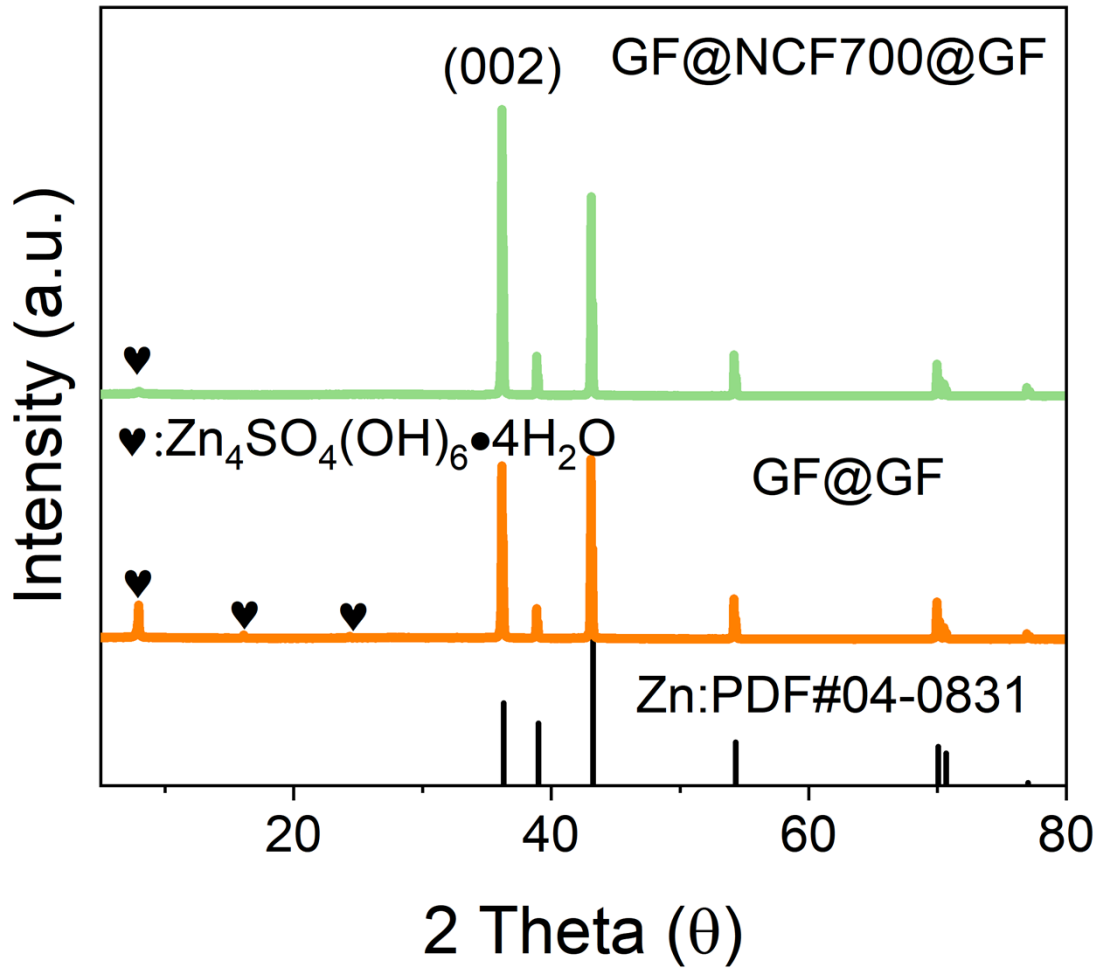
128

129 Fig. S9 The rate performance of symmetrical cells based on GF@GF and
130 GF@NCF700@GF.

131

132

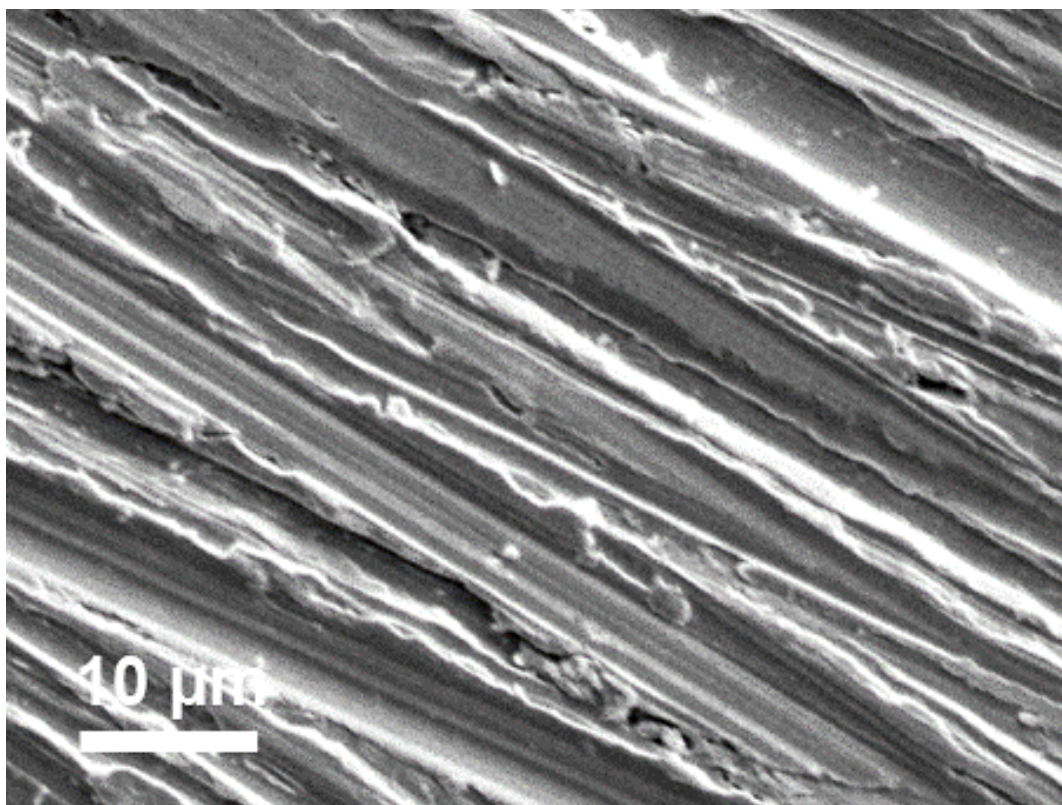
133



134

135 Fig. S10 XRD patterns of Zn anode based on GF@GF and GF@NCF700@GF after
 136 20 cycles..

137

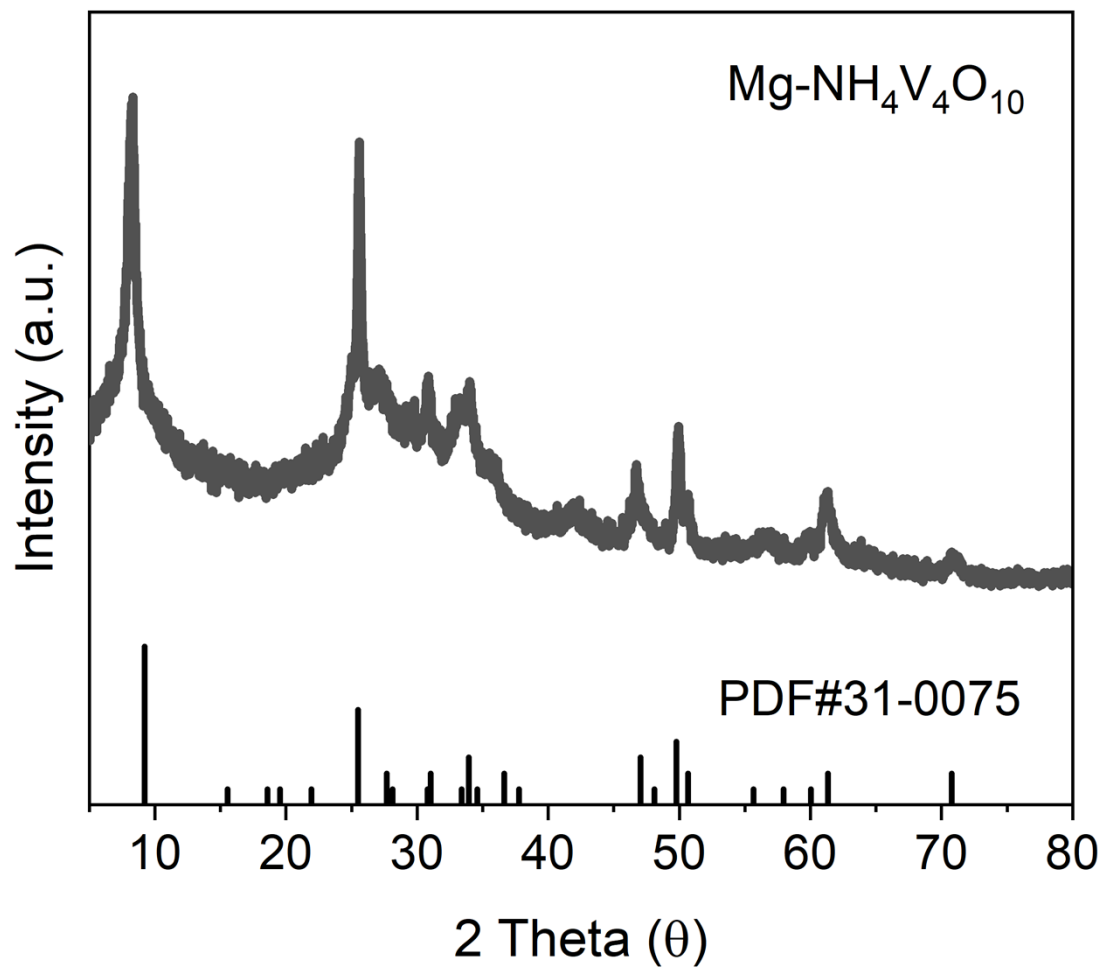


138

139 Fig. S11 SEM image of Zn foil before cycling.

140

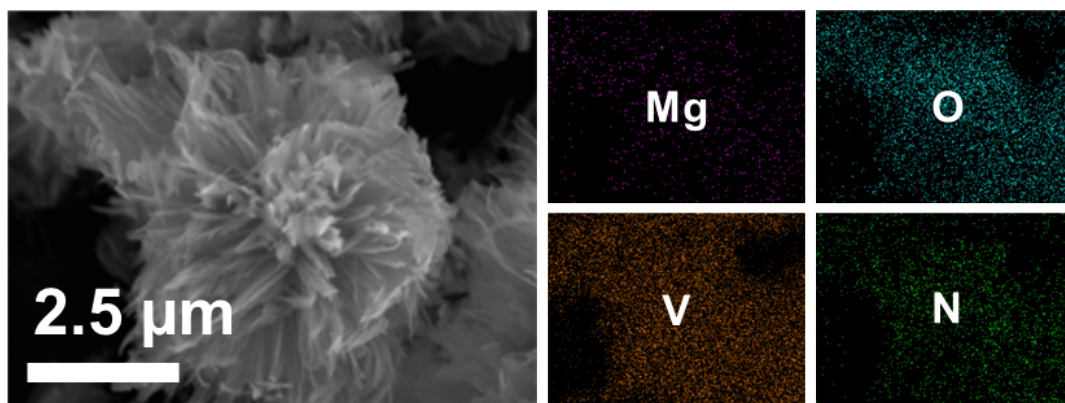
141



142

143 Fig. S12 XRD pattern of MNVO.

144

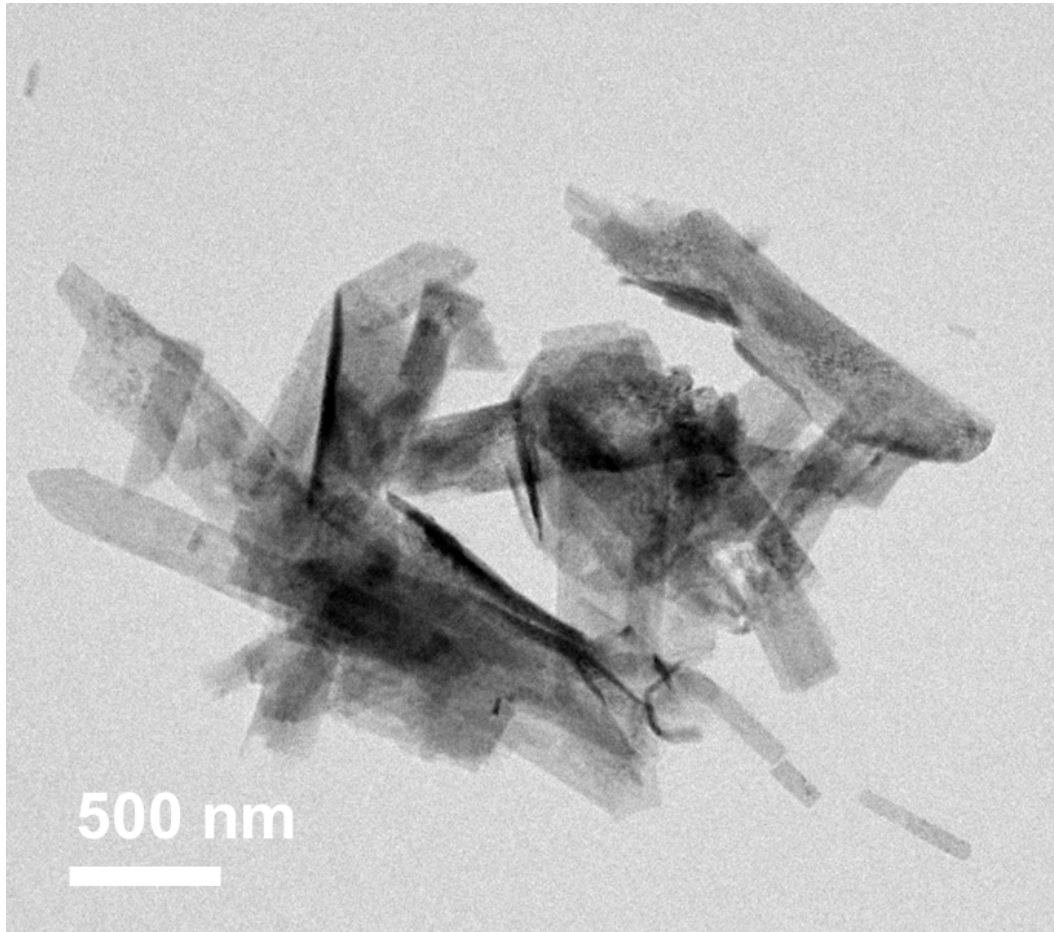


145

146 Fig. S13 SEM image and corresponding EDS mapping of MNVO.

147

148



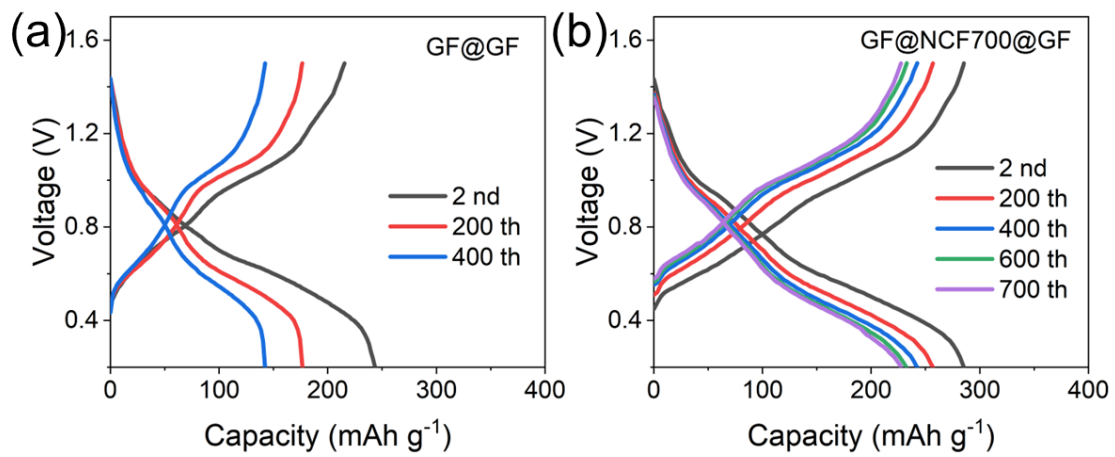
149

150 Fig. S14 TEM image of MNVO.

151

152

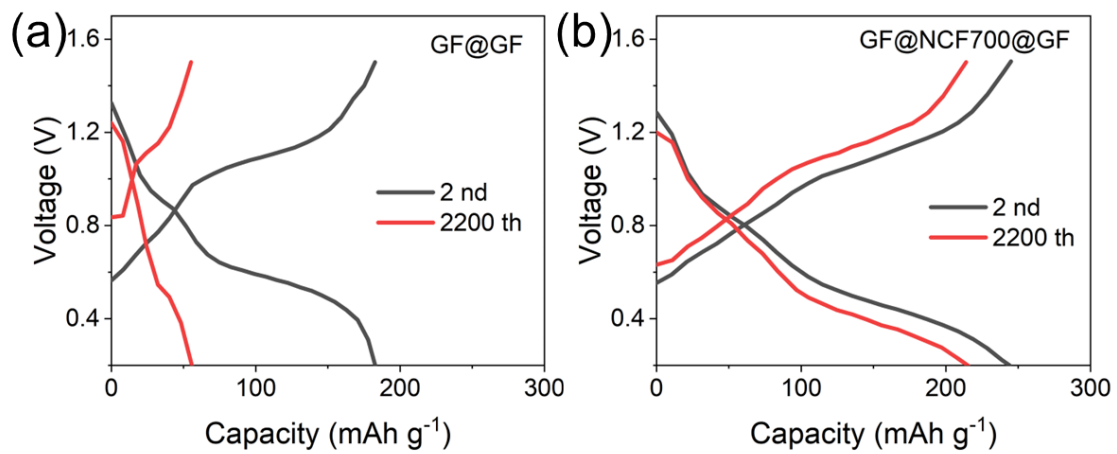
153



154

155 Fig. S15 Galvanostatic charge-discharge curves of (a) Zn||GF@GF||MNVO and (b)
 156 Zn||GF@NCF700@GF||MNVO full cell at 1 A g⁻¹.

157



158

159 Fig. S16 Galvanostatic charge-discharge curves of (a) Zn||GF@GF||MNVO and (b)
 160 Zn||GF@NCF700@GF||MNVO full cell at 3 A g⁻¹.

161

162

163 References

164

165 1 L. Li, Y. Li, Y. Ye, R. Guo, A. Wang, G. Zou, H. Hou and X. Ji, *Acs Nano*, 2021,
166 **15**, 6872-6885.

167 2 X. Wang, Y. Wang, A. Naveed, G. Li, H. Zhang, Y. Zhou, A. Dou, M. Su, Y. Liu,
168 R. Guo and C. C. Li, *Adv. Funct. Mater.*, 2023, **33**, 2306205.

169